bioRxiv preprint doi: https://doi.org/10.1101/018937; this version posted September 15, 2015. The copyright holder for this preprint (which was not certified by peer review) is the author/funder. All rights reserved. No reuse allowed without permission.

# Size structures sensory hierarchy in ocean life

Erik A. Martens[1,2,3,5,♯,*] Navish Wadhwa[1,4,5,♯,†] Nis S. Jacobsen[1,2], Christian Lindemann[2], Ken H. Andersen[1,2], and André Visser[1,2]

[1]*VKR Centre for Ocean Life, Technical University of Denmark, Jægersborg Allé 1, 2920 Charlottenlund, Denmark* [2]*National Institute of Aquatic Resources, Technical University of Denmark, Charlottenlund Slot, Jægersborg Allé 1, DK-2920 Charlottenlund, Denmark* [3]*Department of Biomedical Sciences, Copenhagen University, Blegdamsvej 3, 2200 Copenhagen, Denmark* [4]*Department of Physics, Technical University of Denmark, DK-2800 Kgs. Lyngby, Denmark* [5]*These authors contributed equally to this study.* [♯]*Corresponding authors.*

**Survival in aquatic environments requires organisms to have effective means of collecting information from their surroundings through various sensing strategies. In this study, we explore how sensing mode and range depend on body size. We find a hierarchy of sensing modes determined by body size. With increasing body size, a larger battery of modes becomes available (chemosensing, mechanosensing, vision, hearing, and echolocation, in that order) while the sensing range also increases. This size-dependent hierarchy and the transitions between primary sensory modes are explained on the grounds of limiting factors set by physiology and the physical laws governing signal generation, transmission and reception. We theoretically predict the body size limits for various sensory modes, which align well with size ranges found in literature. The treatise of all ocean life, from unicellular organisms to whales, demonstrates how body size determines available sensing modes, and thereby acts as a major structuring factor of aquatic life.**

Keywords: ocean life, sensing modes, body size, sensing range, fluid physics, traits

## I. INTRODUCTION

The marine pelagic environment is sparsely populated. To survive, organisms must scan volumes of water millions of times their own body volumes per day [1]. While searching is a challenge in itself, there is also the continual risk of predation. The result is a strong evolutionary drive to effectively gather information on the proximity of prey, mates and predators [2]. Here, we examine the means by which this information is gathered by marine pelagic organisms, that is, their sensory ability. In particular, we wish to understand relationships between the size of an organism and the usability of the various types of senses.

Indeed, size is a key parameter to characterize biological processes in marine environments [1, 3–6]. A cursory examination indicates at least some size-dependent organization as to which sensory modes organisms use in the marine pelagic environment. For instance, the smallest organisms (e.g., bacteria) depend heavily on chemical signals, while for larger animals (e.g., copepods), sensing of fluid flows becomes important, too. For even larger organisms, vision (e.g., crustaceans and fish), hearing (e.g., fish) and echolocation (e.g., toothed whales) become increasingly relevant sensory modes (Supplementary Figure 1). How can we understand this pattern on the grounds of physiology and physics using scaling rules, which are the two basic constraints on the workings of any organism [7, 8]? Our aim here is to determine the body size limits of different sensing modes based on physical grounds, and to explain how the sensory hierarchy is structured by size.

* erik.martens@sund.ku.dk
† nawa@fysik.dtu.dk

## II. SENSING AS A PHYSICAL PROCESS

Our goal is to understand how size determines sensory modes available to an organism. We restrict ourselves to those sensory modes that are the primary means of remotely detecting the presence of other organisms: chemosensing of compounds, mechanosensing of flow disturbances provoked by moving animals, image vision in sufficiently lit areas, hearing of sound waves, and their generation for echolocation. We further restrict ourselves to the pelagic zone. All sensing involves an organism and a target; thus, we refer to the *organism* of size $L$ and the *target* of size $L_t$. The two lengths are related via the dimensionless size preference $p = L_t/L$ (we assume $p = 0.1$ for predation, $p = 1$ for mating, $p = 10$ for predator avoidance). Clearly, other modes such as electroreception [9] or magnetoreception [10] may supplement the above mentioned modes, and organisms may switch between sensing modes depending on proximity to the target; here, however, we restrict ourselves to the aforementioned senses and consider them as the predominant primary sensory modes.

It is possible to decompose sensing into three fundamental sub-processes (Figure 1):

***Generation***. Animals emit signals by creating fluid disturbances, creating sounds or reflecting ambient light. The target's features such as its size, $L_t$, affect the signal. Chemosensing, hearing and mechanosensing require a signal or an action from the target, whereas vision and echolocation do not. Echolocation in particular is an 'active sense', as the signal is generated by the organism and hence influenced by organism fea-

bioRxiv preprint doi: https://doi.org/10.1101/018937; this version posted September 15, 2015. The copyright holder for this preprint (which was not certified by peer review) is the author/funder. All rights reserved. No reuse allowed without permission.



tures such as size $L$.

***Propagation***. The distance over which a signal propagates before getting subdued by noise is sensitive to many factors. For instance, the oceans are awash with traces of various chemicals. Detection of a specific compound requires concentrations higher than the background, and depends on its diffusivity, release rate, stability, etc. This distance sets a sensing range $R$.

***Detection***. Is the organism — given the physical constraints — able to build a sensor? This requires a cost-effective mechanism by which information can be collected at a practical level of resolution. Size and complexity of the organism determine this ability.

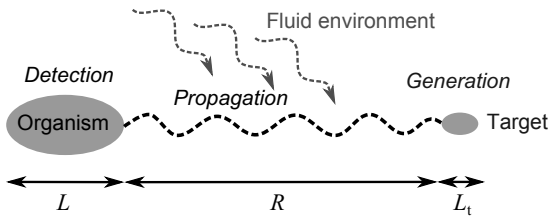


FIG. 1. Schematic of the participants and the processes involved in sensing.

Each of these sub-processes is constrained by size. Thus the length scale imprints itself automatically on the remote detection of other organisms. But limits of the usage of specific sensing modes are not necessarily clear-cut. For instance, in case of vision, the boundary between an image-forming eye (e.g., in fish) and non-image forming 'eye spots' that enable phototaxis (e.g., in copepods, protists) is not sharply defined. Moreover, simultaneous use of multiple senses complicates the situation. We make the simplifying assumption of no integration between senses, and treat them in isolation from each other. Within its limitations, this investigation may not yield exact numbers; it provides *characteristic* body-size limits for the sensory modes and yields valuable understanding of the structure of sensing in marine life, based on first principles.

## III. CHEMOSENSING

The ability to detect chemical compounds is ubiquitous. All life forms have this ability and are equipped with chemosensing apparatuses [11]. Chemotaxis and the use of chemosensing in remote detection can be divided into two modes: i) gradient climbing defined as moving along a gradient towards (or away from) a stationary target, and ii) following a trail laid out by a moving target [12, 13].

### A. Size limits for chemosensing

Gradient climbing ability would be size independent, were it not for two randomizing physical effects. For very small organisms, gradient climbing ability is impaired due to Brownian rotation [14], caused by molecular motions in the fluid. Due to this, the organism cannot direct itself along a gradient using a biased random walk (Figure 2A). This happens for $L$ less than the length scale characteristic of Brownian motion, $L_{\mathrm{Br}}$ ($0.1 - 1\mu$m) [15]. Using a similar argument, Dusenbery [16] has argued that below $L = 0.6$ $\mu$m, directed motility, and thus chemotaxis, is infeasible due to Brownian rotation.

An upper limit for gradient climbing is imposed when turbulence disrupts the smoothness of the chemical gradient, for $L$ greater than the Batchelor scale $L_{\mathrm{B}} \approx (\nu D^2/\varepsilon)^{1/4}$, where $\nu$ is the kinematic viscosity, $D$ the molecular diffusivity, and $\varepsilon$ the turbulent energy dissipation rate. $L_{\mathrm{B}}$ is the length scale at which the diffusion time scale becomes comparable to the dissipation time for the smallest turbulent eddies (Figure 2B). In the ocean, $\varepsilon$ ranges between $10^{-8}$ and $10^{-3}$ m$^2$s$^{-3}$ [17, 18]. $L_{\mathrm{B}}$ is between 5 and 100 $\mu$m in moderate turbulence (for a typical value of $D \sim 10^{-9}$ m$^2$s$^{-1}$), but can become much larger in quiescent environments.

For detecting a moving target that releases a chemical trail, the physical constraints are similar to gradient climbing. For $L$ above the Kolmogorov scale $L_{\mathrm{K}} \approx (\nu^3/\varepsilon)^{1/4}$, directional information in the trail is reduced due to the isotropy in turbulent flows [19], impairing chemotaxis. $L_{\mathrm{K}}$ is around 1 cm in moderate turbulence [17], above which trail following becomes progressively worse. When $L$ is larger than the integral length scale $L_{\mathrm{I}}$, trail following may become effective again as the turbulent trail at this scale is anisotropic (Figure 2C). Typical values for $L_{\mathrm{I}}$ in a stratified ocean are around 1 m or larger [20, 21]. Thus, between $\sim$ 1 cm and $\sim$ 1 m, trail following is impaired, and requires averaging over space and time [22]. Note that in the absence of environmental turbulence, $L_{\mathrm{K}}$ and $L_{\mathrm{I}}$ are determined by the size of the trail source.

### B. Sensing range for chemosensing

Size limits for the functioning of chemosensing also apply to the sensing range. For example, in gradient climbing, the maximal distance up to which a chemical gradient remains uninterrupted is $L_{\mathrm{B}}$. Another factor affecting the range for gradient climbing is the diffusion time scale. For a typical compound to diffuse over $d = 1$ cm, it can take up to days ($t = d^2 D^{-1}$ where $D \sim 10^{-9}$m$^2$s$^{-1}$). This makes the signal irrelevant for many small organisms, because by that time they have moved elsewhere, been preyed upon, or have multiplied several times. Thus, gradient climbing is relevant only up to small distances. Similarly, for trail following, sensing range is limited to $L_{\mathrm{K}}$.

bioRxiv preprint doi: https://doi.org/10.1101/018937; this version posted September 15, 2015. The copyright holder for this preprint (which was not certified by peer review) is the author/funder. All rights reserved. No reuse allowed without permission.



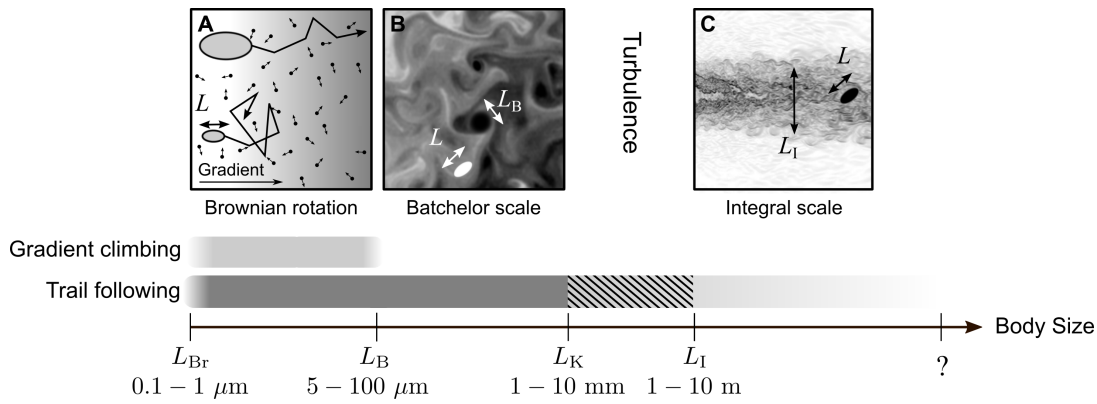


FIG. 2. Body sizes over which chemosensing can be used effectively. A schematic illustration of Brownian rotation (A), Batchelor scale (B), and integral scale (C) is included at the top.

## IV. MECHANOSENSING

Any object moving in fluid generates a hydromechanical disturbance that can potentially be detected with the appropriate sensory apparatus [23]. For many small organisms such as zooplankton [23–25], it is the dominant sensory mechanism. Many fishes, especially in dimly lit environments, also rely heavily on mechanosensing using the lateral line organ [26]. The nature of a fluid disturbance generated by a target of size $L_t$ swimming with a velocity $U_t$ is largely determined by the dimensionless Reynolds number (Re), defined as $\mathrm{Re} = L_t U_t/\nu$, where $\nu$ is the kinematic viscosity [27]. For small Re, such as for most plankton, flow is dominated by viscosity and is laminar [28]. For large Re, such as for large fishes or mammals, inertia dominates, and the flow tends to be turbulent [29].

### A. Propagation of fluid disturbances

For a target passively sinking at low Re in unbounded fluid (e.g., the pelagic zone), the velocity ($u$) induced in the fluid decays with distance $r$ as $u \sim r^{-1}$ [23]. For a self-propelled target, the induced velocity decays as $u \sim r^{-2}$ [23]. Recent studies have shown that for breast-stroke swimming plankton and impulsively jumping copepods, $u$ decays more rapidly as $u \sim r^{-3}$ and $u \sim r^{-4}$, respectively [30, 31]. At high Re, the fluid disturbance generated by a target becomes turbulent, if $L_t$ is much larger than $L_K$, resulting in a turbulent wake.

### B. Detection

Setae on the antennae of a copepod are classic examples of mechanosensors (Supplementary Figure 2). Setae sense velocity difference across their length, and activate when it exceeds a certain threshold $s$ [25], defining setae sensitivity [32], typically between 10 and 100 $\mu$m/s [23]. In unicellular organisms such as ciliates and dinoflagellates, a response occurs above a critical fluid deformation rate [24, 33], equivalent to a threshold velocity difference across the cell. In the lateral lines of fish, the working sensor is a seta-like kinocilium [34]. In general, mechanosensing requires a velocity differential on the organism's body, as a result of fluid deformation. Given a sensitivity $s$ of a mechanosensor of length $b$, embedded in fluid with deformation rate $\Delta$ (measured in $\mathrm{s}^{-1}$), the criterion for detection can be written as

$$\Delta \cdot b > s. \tag{1}$$

### C. Sensing range for mechanosensing

We estimate the sensing range $R$ for the most relevant case of a self-propelled target. For $R \gg b$, Visser [23] has shown that $R \approx (3U_t L_t^2 b/s)^{\frac{1}{3}}$. The swimming velocity of the target is related to its size by the empirical relation $U_t \sim c_1 L_t^{0.79}$ with $c_1 = 6.5\ \mathrm{m}^{0.21}/s$ [1]. For prey detection ($p = 0.1$), assuming that the sensor is about a tenth of the body size ($b = L/10$), we get

$$R \approx c_2 L^{1.26} \tag{2}$$

where $c_2 = 3.98\ \mathrm{m}^{-0.26}$.

From this estimate, a copepod of $L \sim 2$ mm has a prey sensing range of about 1.5 mm. The exact scaling coefficient is determined by the organism's morphology and the swimming characteristics of the target, but equation (2) provides a rough estimate. Like in chemical trail following, an upper limit of mechanosensing range $R$ is set by the Kolmogorov scale, $L_K$, above which turbulence disrupts the signal.

### D. Size limits for mechanosensing

The lower size limit for mechanosensing in the pelagic zone is dictated by inequality (1). We consider the case of a small prey individual detecting a

bioRxiv preprint doi: https://doi.org/10.1101/018937; this version posted September 15, 2015. The copyright holder for this preprint (which was not certified by peer review) is the author/funder. All rights reserved. No reuse allowed without permission.



larger predator ($p$ = 10). For a target (predator) swimming with a velocity $U_t$, fluid deformation scales as $\Delta \sim U_t/L_t$. Using again the empirical scaling of $U_t \sim c_1 L_t^{0.79}$ [1], and further using $L = L_t/10$, we can deduce that

$$\Delta \sim c_3 \cdot L^{-0.21}, \tag{3}$$

where $c_3 = 3.98\ \mathrm{m}^{0.21}\mathrm{s}^{-1}$.

To close the problem, we again use $b = L/10$. Combining (1) and (3), substituting $b$ and using an intermediate value for $s$ = 50 $\mu$m/s, we get a lower size limit of $L > 11$ $\mu$m. Thus we expect the lower size limit for an organism to use mechanosensing in the pelagic zone to be of the order of a few micrometers. Given the sensitivity of mechanosensing apparatuses, smaller organisms are unable to detect the hydromechanical disturbances relevant to their size.

The upper size limit of mechanosensing is prescribed by the same constraints as those for chemical trail following. The generated flows are disintegrated by turbulence at $L > L_K$, rendering mechanosensing progressively less effective above organism sizes of around 1 cm. We also conjecture that like trail following, mechanosensing abilities may improve for organisms larger than the integral length scale $L_I$.

## V. VISION

Simple functions of vision include differentiating light from dark, entrainment to a circadian rhythm [35], and orientation [36], while more complex functions involve navigation, pattern recognition, and food acquisition. Prey and predator detection from some distance requires sufficient image resolution. In general only two fundamental principles are used to build an eye: i) compound eyes, which comprise of a number of individual lenses and photo-receptors laid out on a convex hemispherical surface, ii) camera eyes with one concave photoreceptive surface where an image is projected through an optical unit (pinhole or lens).

### A. Light propagation in the marine environment

Given that a target is lit and visible, the reflected light must travel through seawater to reach the receiving organism. The intensity of light attenuates geometrically with distance $r$ as $r^{-2}$, and more steeply due to the added effects of scattering and absorption by solutes and seston [37]. In general, light intensity along a given path decreases as $e^{-\alpha r}$ where $\alpha$ (measured in $\mathrm{m}^{-1}$) is called the absorption coefficient [38].

### B. Physiological limits to eye size

The resolution of the compound eye is limited by the size of ommatidia (photoreceptor units in compound eyes). They cannot be reduced in size to achieve a resolution better than 1° [39]. Thus, camera eyes, which we consider in the following, outperform compound eyes in compactness [39, 40]. The functioning of a small eye is limited by two constraints. First, a smaller eye captures less light. Second, a smaller eye has lower resolution: the photoreceptive units constitute the smallest components in an eye and are based on opsin molecules, the universally represented light-capturing design in the animal world [41]. Thus, the width of a photoreceptor $d_p \approx 1$ $\mu$m [42] is an absolute limiting factor for any eye design. Therefore, $n$ pixels amount to a retina diameter of $d \approx n^{1/2} d_p$. Considering a minimal required resolution for a usable image-forming eye to be $100^2$ pixels, the corresponding retina would have a diameter $d \approx 0.1$ mm. Depending on the eye-to-body size ratio, this corresponds to an organism of around $L \approx 1$ to 3 mm.

Arguments for an upper size limit for eyes are not evident on physical grounds. The largest known marine animals carry eyes (see Discussion). However, the higher resolution and sensitivity resulting from larger eyes do not necessarily yield a larger sensing range as it may be limited by turbidity, as we discuss next.

### C. Visual range

The visual range of an organism can be estimated by considering the properties of a (pin-hole) camera eye, following an argument by Dunbrack and Ware [43]. We use Weber contrast $C = (I - I_b)/I_b$, where $I$ and $I_b$ are the intensities of the target and the background, respectively. The maximal distance $R$ at which a predator can discern a prey individual of size $L_t$ requires that the apparent contrast $C_a$ of the target matches the contrast threshold of the eye, $C_{th}$. The inherent contrast of the target, $C_0$ declines with distance $r$, yielding [38]

$$C_a = C_0 \cdot e^{-\alpha r}. \tag{4}$$

$C_{th}$ is a declining function of the number of visual elements $n$ involved in perceiving the target:

$$C_{th} = C_{th,min}(z) + K_{ph}/n. \tag{5}$$

This formula is partly based on Ricco's law [44] that expresses the inverse proportionality between $C_{th}$ and $n$, and is supplemented by adding the minimum contrast threshold $C_{th,min}$ to represent saturation of the contrast at a minimal value [45]. $C_{th,min}$ varies in different environments and, in particular, depends on the available backlight at a given depth $z$.

The number of visual elements $n$ involved in image detection is equal to their density, $\sigma$ (measured in $\mathrm{m}^{-2}$), times the projected image area. Assuming $R$ is large relative to the eye ball diameter $L_{eye}$, we can deduce $n = \sigma\pi/4 L_{img}^2 \approx \sigma L_{eye}^2 L_t^2 R^{-2}$ (Supplementary Figure 3). Noting the universal size of the opsin molecule across species, we may assume that $\sigma$ is independent of eye size. Introducing the ratio $a = L_{eye}/L$ [46] and using $p = L_t/L$, we get

bioRxiv preprint doi: https://doi.org/10.1101/018937; this version posted September 15, 2015. The copyright holder for this preprint (which was not certified by peer review) is the author/funder. All rights reserved. No reuse allowed without permission.



$n = \sigma a^2 p^2 L^4 R^{-2}$. The range $R$ is determined by the condition $C_a \geq C_{\text{th}}$:

$$C_0 e^{-\alpha R} \geq C_{\text{th,min}}(z) + K R^2 L^{-4}, \tag{6}$$

where $K = K_{\text{ph}} \sigma^{-1} a^{-2} p^{-2}$ is a constant characterizing the photoreceptor sensitivity, $K_{\text{ph}}/\sigma$, eye-to-body-size ratio, $a$, and size preference, $p$. Sample solutions for the condition $C_a = C_{\text{th}}$ yield the range $R$ at a given body size $L$ (Figure 3A). Isolating $R$ from Eq. (6) is impossible; however, asymptotic solutions can be derived for two limits:

(i) "Clear-water limit": when $\alpha \to 0$, $R$ is limited by the eye's resolution; thus, $R \sim [(C_0 - C_{\text{th,min}})/K]^{1/2} L^2$.

(ii) "Turbid-water limit": when $C_0 - C_{\text{th,min}} \gg K R^2 L^{-4}$; thus, $R \sim (\ln C_0 - \ln C_{\text{th,min}})/\alpha$. $R$ is independent of $L$ and only limited by the sensitivity of a visual element, $C_{\text{th,min}}$.

Generally, the visual range decreases if light is reduced, e.g., at large depth $z$, leading to a higher $C_{\text{th,min}}$ [cases (i),(ii)]; or if the turbidity is strong (larger $\alpha$) [case (ii)]. The cross-over between the two limits occurs when $L \sim L_x \sim \alpha^{-1/2}$ (Supplementary text). The visibility range in pure water for light of 550 nm is theoretically estimated at 74 m [47], and measurements in the open sea range from 44-80 m [48]. The visual range has also been predicted in more elaborate models [49].

## VI. HEARING

Sound propagates through the ocean as pressure waves, resulting in alternating compression and rarefaction of water in regions of high and low pressure, respectively. Any form of hearing must detect sound waves by converting them into vibrations of an organ that stimulates nerve cells. In fishes, sound waves displace sensory hairs against the calcareous *otolith*, and this relative motion is detected. By contrast, in mammalian ears, sound waves excite the tympanic membrane (ear-drum), the motion of which is sensed by ciliary hairs in the cochlea.

Most sounds relevant to ocean life, except echolocation, fall into the range of a few hertz up to a few kilohertz. Sounds generated by marine animals due to rapid movements or for communication, have frequencies rarely exceeding 1 kHz [50]. Communication by marine mammals usually consists of a burst of clicks or of whistles (4-12 kHz), while the echolocating signals of odontoceti range between 20 and 200 kHz [51].

### A. Underwater sound propagation

As sound waves travel through a medium, sound intensity attenuates with distance from the target $r$, due to two processes: (i) geometric spreading ($r^{-2}$ in open space), and (ii) absorption in water. The latter is frequency dependent: 1 dB/km at 10 kHz, but only $10^{-4}$ dB/km at 100 Hz in seawater[1] [38]. Sound is therefore only weakly attenuated in seawater, and it can potentially carry information over large distances.

### B. Lower limit for sound detection

Detection of sound requires either an organ of significantly different density than that of water (e.g., the otolith), or a large detector array (e.g., auricle and drum), to allow detection by responding to spatial gradients of particle displacement [38]. A density contrast organ such as the otolith has to move relative to the surrounding fluid, as explained above. Motions in small sound-sensing organs (operating at low *Re*) are inherently more damped by viscosity than larger ones, impairing the practicality of sound detection by small organisms. Without high density contrast in the hearing organ, the detector array and thus the organism would have to be at least as long as the wavelength of sound (15 cm at 10 kHz). Thus hearing – with or without a density contrast organ – is impractical for pelagic organisms smaller than a few centimetres.

Many fishes have swim bladders (sometimes connected to the otolith-containing cavity through bony connections called the *Weberian ossicles*) that transduce pressure waves to mechanical motion and act as displacement amplifiers for sound via resonance [38, 52]. Similarly, odontocetes use the fat-filled bones of their lower jaw as an amplifying cavity [51]. Swim bladders are air-filled structures that amplify sound maximally when in natural resonance with the sound waves [38]. Frequencies very different from the resonance frequency of the swim bladder do not amplify well, and may even be damped if too different [38]. Based on an assumption of a spherical, air-filled swim bladder, the resonance frequency, $f$, can be approximated [38] as

$$f = \frac{1}{2\pi r_{\text{b}}} \sqrt{\frac{3\Gamma P}{\rho}}, \tag{7}$$

where $P$ is the depth-dependent hydrostatic pressure, $r_{\text{b}}$ the radius of the swim bladder, $\rho$ the density of sea water, and $\Gamma$ the adiabatic exponent ($\sim 1.4$ for air); $r_{\text{b}}$ is typically around 5-10 % [53] of the body size $L$ of the fish. Using $r_{\text{b}} = L/10$ for a conservative estimate, $L$ would need to be at least 3 cm at the sea surface, in order to amplify the high-frequency end (1 kHz) of the ambient underwater sound spectrum, and $L = 11$ cm at a depth of 100 m (Figure 3B). To hear the more typical lower frequencies, $L$ would have to be larger still. Thus, we approximate that the lower body size limit for detection of sound using swim bladders is around a few centimetres.

[1] The decibel level is defined via $I_{\text{dB}} = 10 \log_{10}(I/I_0)$, where $I$ is the sound intensity and $I_0$ is a reference frequency.

bioRxiv preprint doi: https://doi.org/10.1101/018937; this version posted September 15, 2015. The copyright holder for this preprint (which was not certified by peer review) is the author/funder. All rights reserved. No reuse allowed without permission.



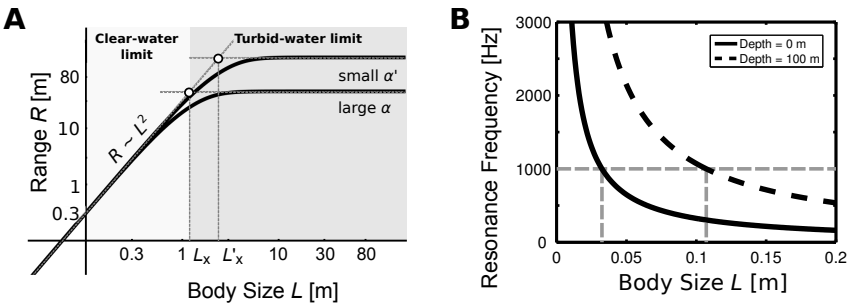


FIG. 3. **A**: Visual sensing range scales with body size, $L$, as $R \sim L^2$ in the clear-water limit ($L \ll L_x$) and as $R \sim$ constant in the turbid-water limit ($L \gg L_x$). Parameters are $C_0 = 0.3, C_{\mathrm{th,min}} = 0.05$ (adopted from [43]), $K = 2.5 \times 10^{-4}$ m$^2$, $\alpha = 0.04$ m$^{-1}$ [69] (and $\alpha' = 0.01$ m$^{-1}$ for comparison). **B**: Relationship of body size and resonance frequency based on Equation (7) and using a swim bladder size $r_b = L/10$ for an individual at the surface (solid curve) and at 100 m depth (dashed curve). The dashed (grey) horizontal line indicates 1 kHz, below which most sounds generated by marine life are found.

## VII. ECHOLOCATION

Echolocation is an active sensing mode, in which the organism emits clicks in the ultrasonic range and interprets the environment based on the echoes of these clicks. Echolocation is common in odontocetes (toothed whales) and is generally used for orientation and prey detection. The generation of echolocating signals in toothed whales is associated with the nasal passage leading up to the blowhole and takes place in the phonic lips. Taking into account the anatomical structures, the dominant frequency can be estimated as the resonance frequency of a Helmholtz oscillator [54]. The diffraction limit sets a resolution limit to $\lambda/2\pi$, where $\lambda$ is the characteristic wavelength of the click [38]. Odontocetes produce clicks with peak energies at frequencies in the range of 20 to 200 kHz [51], the resulting resolution lies between 1 to 8 mm. Using an intermediate value (5 mm), and assuming that the target is at least one order of magnitude larger than the smallest resolvable feature, we get a minimal target size of 50 mm. Echolocation is typically used for prey detection, so $p = 0.1$. Thus we get a lower body size limit for an echolocating organism to be $L \approx 500$ mm. It also implies that objects smaller than about 1 mm do not scatter sound signals in the frequency range we are considering, allowing echolocation to be useful in turbid waters where vision is severely restricted.

### A. Sensing range

The generated acoustic signal first travels through water, is then partially reflected by the target, and the remainder of the signal (minus attenuation) travels back to the organism. Emitted sound intensity, $I_e$, is thus reduced by the processes of reflection and geometric divergence, causing signal intensity to attenuate as $(2r)^{-2}e^{-2\mu r}$. The strength of the returned signal must exceed the threshold intensity for detection in the ear, $I_r = I_0$. Assuming that ear threshold sensitivity is independent of $L$, but that emitted sound intensity $I_e$ and carrier frequency scale with $L$, the sensing range can be estimated as (Supplementary Text for details)

$$R \sim p I_0^{-1/2} L^{\gamma}, \tag{8}$$

where $p = L_t/L$ is the size preference ratio and the exponent $\gamma$ lies between 2.125 to 2.5 that compares reasonably well with data. The scaling factor can be estimated from data describing the echolocation range of small marine mammals (Supplementary Text).

## VIII. DISCUSSION

We have attempted to synthesize an understanding of how physiology and the physical environment enable and constrain an aquatic organism's ability to gather information from its surroundings. By reducing the relevant physical mechanisms to their simplest forms, we have identified the most pressing constraints on the functioning of various senses. Our goal has been to explain the transition from one dominant sense to another with changing body size, as observed in nature. A comparison of the predicted size limits with those observed in nature supports our analysis (Table I, Figure 4). The predicted size ranges correspond well with known minimal and maximal sizes of animals using a specific sense. Size limits of a sense do not imply that an organism cannot detect the signal outside the limits at all, but rather that beyond these limits, the usefulness of the sense is compromised in comparison with other senses.

We could not conceive any upper size limits on physical grounds for chemosensing, mechanosensing, hearing, and vision. Indeed, the largest known organism in the ocean, the blue whale ($L = 30$ m), is known to use all of these senses. Chemosensing is the only sense available to the smallest organisms, and its theoretical lower size limit ($L_{\mathrm{Br}} \sim 10^{-7} - 10^{-6}$ m) is consistent with the smallest known motile organisms (bacteria, $L = 0.8$ $\mu$m [16]). Chemosensing is presumably slightly impaired due to turbulence in intermediate size ranges, in which integration of multiple senses such

bioRxiv preprint doi: https://doi.org/10.1101/018937; this version posted September 15, 2015. The copyright holder for this preprint (which was not certified by peer review) is the author/funder. All rights reserved. No reuse allowed without permission.



TABLE I. Lower and upper size (body length) limits for various senses. Predicted theoretical limits denote orders of magnitude.

| | Observed limit | | | | Theoretical limit | |
|---|---|---|---|---|---|---|
| | Lower [m] | | Upper [m] | | Lower [m] | Upper [m] |
| Chemosensing | $8 \cdot 10^{-7}$ | [16] | 30 | [55] | $\sim 10^{-7}$ | — |
| Mechanosensing | $7 \cdot 10^{-6}$ | [56] | 30 | [55] | $\sim 10^{-5}$ | — |
| Vision | $1.5 \cdot 10^{-3}$ | [57] | 30 | [55] | $\sim 10^{-3}$ | — |
| Hearing | $9 \cdot 10^{-3}$ | [58] | 30 | [55] | $\sim 3 \cdot 10^{-2}$ | — |
| Echolocation | 0.55 | [59] | 18.6 | [60] | $\sim 0.5$ | — |

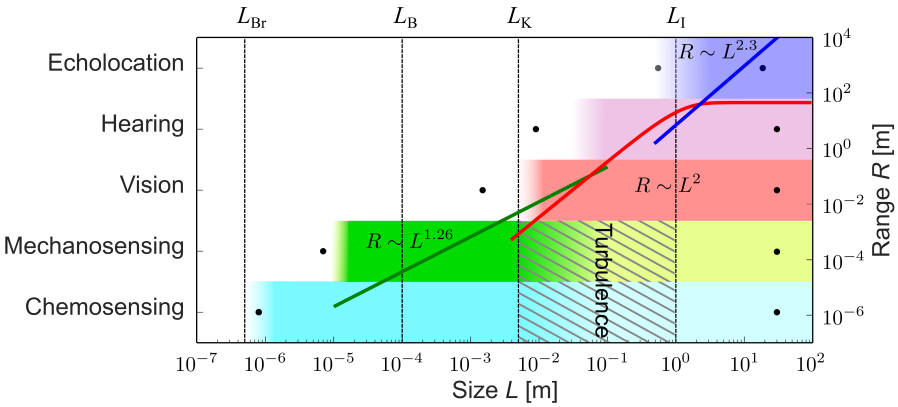


FIG. 4. Upper and lower body size limits and ranges for different senses. Dots denote the largest and smallest sizes known to employ a given sense, and shaded rectangles show the theoretical estimates of the size range in which a sense is expected to work. Green, red, and blue curves show the theoretical scaling of sensing range with size for mechanosensing, vision, and echolocation, respectively.

as mechanosensing and vision might be very useful. Chemosensing for trail following is an important sensory mode for large bony fishes [61] and sharks [62], which have sizes larger than $L_I$.

The theoretical lower limit for mechanosensing in the pelagic environment is a few micrometers, in the realm of protists; to our knowledge, marine protists sized 7-10 $\mu$m are the smallest pelagic organisms known to use mechanosensing [56]. However, it is only the lower limit for pelagic zones; smaller bacteria are known to be able to sense mechanical stresses when getting in contact with a solid body [63]. Large copepods and small fish occupy the size range where mechanosensing starts becoming less effective. Its use by fish is demonstrated in many species using lateral lines to find prey and sense flows [26]. Larger fish receive a poorer signal quality due to turbulence, and for this reason some larger sharks are known not to use lateral lines for prey detection [64]. Some marine mammals (seals and sea lions) have the ability to follow turbulent trails using their mystacial vibrissae [65], likely due to being larger than the integral length scale set by the target.

The camera eye takes records for both the smallest and the largest eye: the smallest image forming eyes (and body sizes) are found in the fish *Schindleria brevipinguis* ($L \approx 7$ mm [66]), and the pygmy squids ($L \approx 1.5$ mm [57]), which compares well with our predicted size limit[2]. The largest known eye belongs to the giant squid, featuring eye-balls up to 30 cm in diameter [67]. Eyes are also found in the largest known species (whales), implying that there is no upper body size limit for image-forming vision in marine animals.

For hearing, the theoretical lower body size limit is found to be a few centimetres. Some fishes are able to manipulate the resonance frequency of swim bladders by changing their membrane elasticities [68]. By hearing outside the resonance frequency, fish larvae of a few millimetres ($L \approx 9$ mm) have been shown to react to sounds [58]. Note that these fishes inhabit shallower waters, where hearing is feasible at smaller sizes (Figure 3B). For echolocation, the predicted lower limit ($\sim$ 0.5 m) is close to the observed smallest size among echolocating marine mammals (Commerson's dolphin, [59]).

Upper limits of sensing ranges are dictated by degradation of signal-to-noise ratios via absorption, geometric spreading (divergence), or environmental disturbances. For chemical gradient climbing and mechanosensing, the signals are randomized beyond a characteristic distance given by $L_B$ and $L_K$, respectively. For mechanosensing the range scales as $R \sim L^{1.26}$ (Figure 4). When mechanosensing can no longer extend its range, vision becomes a viable solution. Visual sensing range in clear water scales as $R \sim L^2$, but cannot exceed the limit set by turbidity. Even in clear waters, vision cannot exceed the range of roughly

[2] The smallest compound eyes are found in the genus *Daphnia*, but their image quality is questionable, see Supplementary Text.

bioRxiv preprint doi: https://doi.org/10.1101/018937; this version posted September 15, 2015. The copyright holder for this preprint (which was not certified by peer review) is the author/funder. All rights reserved. No reuse allowed without permission.



80 m. Here, vision may be complemented by hearing and echolocation mainly because sound is capable of travelling large distances in sea-water without significant attenuation. Although we could not develop a scaling for hearing range, we could determine the sensing range of echolocation, which scales approximately as $R \sim L^{2.3}$ and is as large as kilometres for larger organisms, comparing well with the known range of marine mammals.

The question arises whether there is a general pattern underlying the size structure of primary sensory modes. For instance, can the transitions between senses be related to metabolic demand? Kleiber's law requires that an organism consumes energy at a rate proportional to $L^{9/4}$[3]. This demand must be fulfilled by maintaining a sufficient clearance rate [4], a function of the swimming velocity $V \sim L^x$ and sensing range $R \sim L^y$ with positive exponents $x, y$. Thus, the clearance rate also increases with $L$. The exponent $y$ appears to increase going up the senses axis (Figure 4). With increasing size and metabolic expenditure, an evolutionary pressure arises to extend the sensing range by investing into a more effective sensory strategy, causing the transition from one to the other primary sensing mode. However, rather than being governed by cost efficiency, it seems more plausible that the transitions between senses are set by the physical limitations of signal generation, transmission and reception. To exemplify, carrying larger eyes can improve resolution and thus extend the sensing range, but beyond a critical (eye) size, increased performance is rendered ineffective due to the clear water limit of the visual range. So a transition is necessitated by the required increase in sensing range, achieved by echolocation.

We have combined biological knowledge, physiology and physics to describe the abilities of the sensory modes in ocean life, from bacteria to whales. Our treatise demonstrates how body size determines available sensing modes, and thereby acts as a major structuring factor of aquatic life. When interpreting the scalings and limits we propose, note that our purpose is to provide first-order approximations based on first principles. Further research is needed to evaluate each of the senses in more detail and to gather more data to examine the arguments presented here. We hope that this work may serve as a starting point for future explorations on sensory modalities and their hierarchical structures.

## AUTHOR CONTRIBUTIONS

EAM and NW contributed equally to the study, collected data, developed models, and wrote the manuscript. NSJ, CL, KHA and AV collected data and helped drafting the manuscript. All authors participated in the design of the study and gave final approval for publication.

## ACKNOWLEDGMENTS

We thank Hanna Rademaker, Julia Dölger and Anders Andersen for helpful discussions, and Thomas Kiørboe for comments on the manuscript. We thank anonymous reviewers for helpful comments that improved the manuscript. The Centre for Ocean Life is a VKR center of excellence supported by the Villum foundation (EAM, NW, CL, NSJ, KHA, AV). The work is part of the Dynamical Systems Interdisciplinary Network, University of Copenhagen (EAM). Partial financial support for CL was provided by EURO-BASIN (FP7, Ref. 264933).

[1] Thomas Kiørboe. How zooplankton feed: Mechanisms, traits and trade-offs. *Biological Reviews*, 86:311–339, 2011.

[2] David B Dusenbery. *Sensory ecology: how organisms acquire and respond to information*. WH Freeman, New York, 1992.

[3] Max Kleiber. Body size and metabolism. *Hilgardia*, 6:315–351, 1932.

[4] KH Andersen and JE Beyer. Asymptotic size determines species abundance in the marine size spectrum. *Am. Naturalist*, 168(1), May 2006.

[5] KH Andersen, Goncalves RJ Berge, T, M Hartvig, J Heuschele, S Hylander, NS Jacobsen, C Lindemann, EA Martens, AB Neuheimer, K Olsson, A Palacz, F Prowe, J Sainmont, SJ Traving, AW Visser, N Wadhwa, and T Kiørboe. Characteristic sizes of life in the oceans, from bacteria to whales. *Annual Review of Marine Sciences*, 8:125, 2016.

[6] David B Dusenbery and Terry W Snell. A critical body size for use of pheromones in mate location. *Journal of Chemical Ecology*, 21(4):427–438, 1995.

[7] David B Dusenbery. Physical constraints in sensory ecology. In FriedrichG. Barth and Axel Schmid, editors, *Ecology of Sensing*, pages 1–17. Springer Berlin Heidelberg, 2001.

[8] David B Dusenbery. *Living at micro scale: the unexpected physics of being small*. Harvard University Press, 2009.

[9] Shaun P Collin and Darryl Whitehead. The functional roles of passive electroreception in non-electric shes. *Animal Biology*, 54(1):1–25, 2004.

[10] Sönke Johnsen and Kenneth J Lohmann. The physics and neurobiology of magnetoreception. *Nature Reviews Neuroscience*, 6(9):703–712, 2005.

[11] Julius Adler. Chemotaxis in bacteria. *Science*, 153(3737):708–716, 1966.

[12] Paul A. Moore, David M. Fields, and Jeannette Yen. Physical constraints of chemoreception in foraging copepods. *Limnology and Oceanography*, 44:166–177, 1999.

[13] John C. Andrews. Deformation of the active space in the low reynolds number feeding current of calanoid copepods. *Canadian Journal of Fisheries and Aquatic*

bioRxiv preprint doi: https://doi.org/10.1101/018937; this version posted September 15, 2015. The copyright holder for this preprint (which was not certified by peer review) is the author/funder. All rights reserved. No reuse allowed without permission.



*Sciences*, 40(8):1293–1302, 1983.

[14] HC Berg. A physicist looks at bacterial chemotaxis. In *Cold Spring Harbor Symposia on Quantitative Biology*, volume 53, pages 1–9, 1988.

[15] James G Mitchell. The influence of cell size on marine bacterial motility and energetics. *Microbial ecology*, 22(1):227–238, 1991.

[16] David B Dusenbery. Minimum size limit for useful locomotion by free-swimming microbes. *Proceedings of the National Academy of Sciences*, 94(20):10949–10954, 1997.

[17] Javier Jiménez. Oceanic turbulence at millimeter scales. *Scientia Marina*, 61:47–56, 1997.

[18] AW Visser, H Saito, E Saiz, and T Kiørboe. Observations of copepod feeding and vertical distribution under natural turbulent conditions in the north sea. *Marine Biology*, 138(5):1011–1019, 2001.

[19] Hendrik Tennekes and John Leask Lumley. *A first course in turbulence*. MIT press, Cambridge, MA, 1972.

[20] H Yamazaki, DL Mackas, and KL Denman. Coupling small-scale physical processes with biology. *The sea: Biological-Physical Interactions in the Ocean*, 12:51–112, 2002.

[21] AW Visser. Small, wet & rational: Individual based zooplankton ecology. Kongens Lyngby, Denmark: Technical University of Denmark, 2010.

[22] Massimo Vergassola, Emmanuel Villermaux, and Boris I Shraiman. 'Infotaxis' as a strategy for searching without gradients. *Nature*, 445(7126):406–409, January 2007.

[23] AW Visser. Hydromechanical signals in the plankton. *Marine Ecology Progress Series*, 222:1–24, 2001.

[24] HH Jakobsen. Escape response of planktonic protists to fluid mechanical signals. *Marine Ecology Progress Series*, 214:67–78, 2001.

[25] J Yen, PH Lenz, DV Gassie, and DK Hartline. Mechanoreception in marine copepods: Electrophysiological studies on the first antennae. *Journal of Plankton Research*, 14:495–512, 1992.

[26] JC Montgomery. Lateral line detection of planktonic prey. In Sheryl Coombs, Peter Görner, and Heinrich Münz, editors, *The Mechanosensory Lateral Line*, pages 561–574. Springer New York, 1989.

[27] Constantine Pozrikidis. *Introduction to Theoretical and Computational Fluid Dynamics*. Oxford University Press, Oxford, UK, 2nd edition, 2011.

[28] Eric Lauga and Thomas R Powers. The hydrodynamics of swimming microorganisms. *Reports on Progress in Physics*, 72(9):096601, September 2009.

[29] George Keith Batchelor. *An introduction to fluid dynamics*. Cambridge University Press, Cambridge, UK, 1967.

[30] Houshuo Jiang and Thomas Kiørboe. The fluid dynamics of swimming by jumping in copepods. *Journal of the Royal Society Interface*, 8:1090–1103, 2011.

[31] Thomas Kiørboe, Houshuo Jiang, Rodrigo Javier Gonçalves, Lasse Tor Nielsen, and Navish Wadhwa. Flow disturbances generated by feeding and swimming zooplankton. *Proceedings of the National Academy of Sciences*, 111(32):11738–11743, 2014.

[32] Thomas Kiørboe and Andre Visser. Predator and prey perception in copepods due to hydromechanical signals. *Marine Ecology-Progress Series*, 179:81–95, 1999.

[33] Elisa M. Maldonado and Michael I. Latz. Shear-stress dependence of dinoflagellate bioluminescence. *The Biological Bulletin*, 212(3):242–249, 2007.

[34] Horst Bleckmann. Role of the lateral line in fish behaviour. In Tony J. Pitcher, editor, *The Behaviour of Teleost Fishes*, pages 177–202. Springer US, 1986.

[35] Georg Kreimer. The green algal eyespot apparatus: a primordial visual system and more? *Current genetics*, 55(1):19–43, February 2009.

[36] Gáspár Jékely, Julien Colombelli, Harald Hausen, Keren Guy, Ernst Stelzer, François Nédélec, and Detlev Arendt. Mechanism of phototaxis in marine zooplankton. *Nature*, 456(7220):395–9, November 2008.

[37] Bogdan Wozniak and Jerzy Dera. *Light Absorption in Sea Water*. Springer New York, New York, NY, USA, 2007.

[38] Mark W Denny. *Air and water: the biology and physics of life's media*. Princeton University Press, 1993.

[39] MF Land. Visual acuity in insects. *Annual Review of Entomology*, 42(46):147–177, 1997.

[40] HB Barlow. The size of ommatidia in apposition eyes. *Journal of Experimental Biology*, (May):667–674, 1952.

[41] MF Land and RD Fernald. The evolution of eyes. *Annual review of neuroscience*, 15(1990):1–29, January 1992.

[42] Helga Kolb, Ralph Nelson, Eduardo Fernandez, and Bryan Jones. Part ii: Anatomy and physiology of the retina: Photoreceptors. In *WEBVISION: The organization of the Retina and Visual System*. 2014.

[43] RL Dunbrack and DM Ware. Energy constraints and reproductive trade-offs determining body size in fishes. In P. Calow, editor, *Evolutionary Physiological Ecology*, pages 191–218. Cambridge University Press, 1987.

[44] Steven Schwartz. *Visual perception: A Clinical Orientation*. McGraw-Hill Professional, 3rd edition, 2004.

[45] D Northmore, FC Volkmann, and D Yager. Vision in fishes: colour and pattern. In *The Behavior of Fish and Other Aquatic Animals*, ed. D. I. Mostofsky, New York: Academic Press, pp 79-136, 1978.

[46] Howard C Howland, Stacey Merola, and Jennifer R Basarab. The allometry and scaling of the size of vertebrate eyes. *Vision research*, 44(17):2043–65, January 2004.

[47] Raymond C Smith and Karen S Baker. Optical properties of the clearest natural waters (200-800nm). *Applied Optics*, 20(2):177–184, 1981.

[48] RJ DaviesColley and DG Smith. Optically pure waters in Waikoropupu ('Pupu') Springs, Nelson, New Zealand. *New Zealand Journal of Marine and Freshwater Research*, 29(2):251–256, 1995.

[49] DL Aksnes and J Giske. A theoretical model of aquatic visual feeding. *Ecological Modelling*, 67(2-4):233–250, June 1993.

[50] AO Kasumyan. Sounds and sound production in fishes. *Journal of Ichthyology*, 48(11):981–1030, December 2008.

[51] DR Ketten. The marine mammal ear: specializations for aquatic audition and echolocation. *The evolutionary biology of hearing*, pages 717–750, 1992.

[52] AD Hawkins. The Behaviour of Teleost Fishes. In *The behaviour of teleost fishes*, ed. Tony J. Pitcher, page 11451, New York, NY: Springer, 1986.

[53] JHS Blaxter. The swimbladder and hearing. In *Hearing and sound communication in fishes*, pp. 6171., eds. WN Tavolga, AN Popper, RR Fay, New York NY: Springer, 1981.

bioRxiv preprint doi: https://doi.org/10.1101/018937; this version posted September 15, 2015. The copyright holder for this preprint (which was not certified by peer review) is the author/funder. All rights reserved. No reuse allowed without permission.



[54] JL Aroyan, MA McDonald, SC Webb, JA Hildebrand, D Clark, JT Laitman, and JS Reidenberg. Acoustic models of sound production and propagation. In Hearing by whales and dolphins (eds. WWL Au, AN Popper, RR Fay), New York NY: Springer, 2000

[55] C Lockyer. Body weights of some species of large whales. *Journal du Conseil*, 36(3):259–273, 1976.

[56] HH Jakobsen, LM Everett, and SL Strom. Hydromechanical signaling between the ciliate mesodinium pulex and motile protist prey. *Aquatic microbial ecology*, 44(2):197–206, 2006.

[57] A Reid. Family idiosepiidae. In *Cephalopods of the world: an annotated and illustrated catalogue of cephalopod species known to date, Vol. I*, pp. 208210, Number 4, Vol 1, eds. P. Jereb and C. F. E. Roper, Rome: FAO, 2005.

[58] KJ Wright, DM Higgs, and JM Leis. Ontogenetic and interspecific variation in hearing ability in marine fish larvae. *Marine Ecology Progress Series*, 424:1–13, March 2011.

[59] BE Joseph, JE Antrim, and LH Cornell. Commerson's dolphin (cephalorhynchus commersonii): a discussion of the first live birth within a marine zoological park. *Zoo biology*, 77:69–77, 1987.

[60] Stephanie L Watwood, Patrick J O Miller, Mark Johnson, Peter T Madsen, and Peter L Tyack. Deep-diving foraging behaviour of sperm whales (physeter macrocephalus). *The Journal of animal ecology*, 75(3):814–25, 2006.

[61] Svein Løkkeborg. Feeding behaviour of cod, *gadus morhua*: activity rhythm and chemically mediated food search. *Animal behaviour*, 56(2):371–378, 1998.

[62] Robert E Hueter, David A Mann, Karen P Maruska, Joseph A Sisneros, and Leo S Demski. Sensory biology of elasmobranchs. In *Biology of sharks and their relatives*, (eds. JC Carrier, JA Musick, MR Heithaus), Boca Raton FL: CRC Press, pages 325–368, 2004.

[63] Pavel Aprikian, Gianluca Interlandi, Brian A. Kidd, Isolde Le Trong, Veronika Tchesnokova, Olga Yakovenko, Matt J. Whitfield, Esther Bullitt, Ronald E. Stenkamp, Wendy E. Thomas, and Evgeni V. Sokurenko. The bacterial fimbrial tip acts as a mechanical force sensor. *PLoS Biol*, 9(5):e1000617, 05 2011.

[64] JM Gardiner and J Atema. Flow sensing in sharks: Lateral line contributions to navigation and prey capture. In Horst Bleckmann, Joachim Mogdans, and Sheryl L. Coombs, editors, *Flow Sensing in Air and Water*, pages 127–146. Springer Berlin Heidelberg, 2014.

[65] Wolf Hanke, Sven Wieskotten, Benedikt Niesterok, Lars Miersch, Matthias Witte, Martin Brede, Alfred Leder, and Guido Dehnhardt. Hydrodynamic perception in pinnipeds. In Cameron Tropea and Horst Bleckmann, editors, *Nature-Inspired Fluid Mechanics*, volume 119 of *Notes on Numerical Fluid Mechanics and Multidisciplinary Design*, pages 255–270. Springer Berlin Heidelberg, 2012.

[66] W Watson and HJ Walker jr. The world's smallest vertebrate, schindleria brevipinguis, a new paedomorphic species in the family schindleriidae (perciformes: Gobioidei). *Records of the Astralian Museum*, 56:139–142, 2004.

[67] MF Land and DE Nilsson. *Animal eyes*. Oxford University Press, 2002.

[68] C Feuillade and RW Nero. A viscous-elastic swimbladder model for describing enhanced-frequency resonance scattering from fish. *The Journal of the Acoustical Society of America*, 103(6):3245–3255, 1998.

[69] Aike Beckmann and Inga Hense. Beneath the surface: Characteristics of oceanic ecosystems under weak mixing conditions – a theoretical investigation. *Progress in Oceanography*, 75(4):771–796, December 2007.

bioRxiv preprint doi: https://doi.org/10.1101/018937; this version posted September 15, 2015. The copyright holder for this preprint (which was not certified by peer review) is the author/funder. All rights reserved. No reuse allowed without permission.

# Supplementary Information: Size Structures Sensory Hierarchy in Ocean Life

Erik A. Martens[1,2,3,5,♯,*] Navish Wadhwa[1,4,5,♯,†] Nis S. Jacobsen[1,2], Christian Lindemann[2], Ken H. Andersen[1,2], and André Visser[1,2]

[1]*VKR Centre for Ocean Life, Technical University of Denmark, Jægersborg Allé 1, 2920 Charlottenlund, Denmark* [2]*National Institute of Aquatic Resources, Technical University of Denmark, Charlottenlund Slot, Jægersborg Allé 1, DK-2920 Charlottenlund, Denmark* [3]*Department of Biomedical Sciences, Copenhagen University, Blegdamsvej 3, 2200 Copenhagen, Denmark* [4]*Department of Physics, Technical University of Denmark, DK-2800 Kgs. Lyngby, Denmark* [5]*These authors contributed equally to this study.* [♯]*Corresponding authors.*

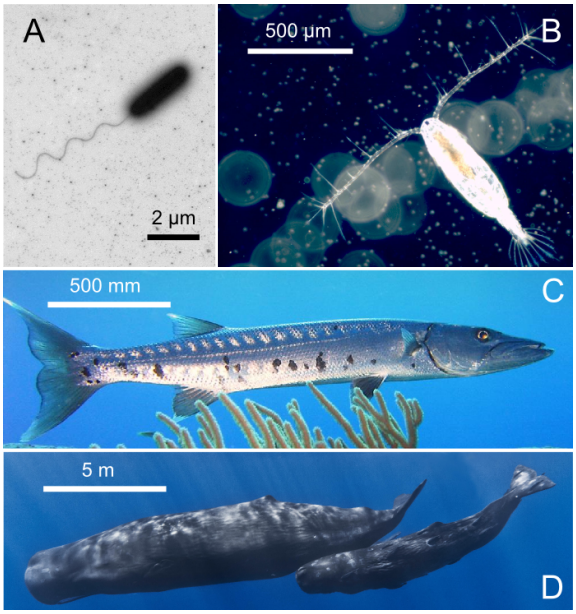


FIG. 1. **Dominant sensing modes** change with increasing size of the organism: (**A**) Small organisms like bacteria (e.g., *Vibrio alginolyticus*) use chemosensing, and move up or down the gradients of chemicals (image courtesy Kwangmin Son and Roman Stocker, MIT). (**B**) Millimetre sized organisms like copepods (e.g. *Acartia tonsa*) use hydromechanical signals to detect predators and prey in the vicinity (image courtesy of Thomas Kiørboe, DTU). (**C**) Larger organisms like fish ( e.g. great barracuda *Sphyraena barracuda*) are often visual predators. (**D**) Toothed whales (e.g. *Physeter macrocephalus*) use echolocation. Images in panels C,D are in public domain.

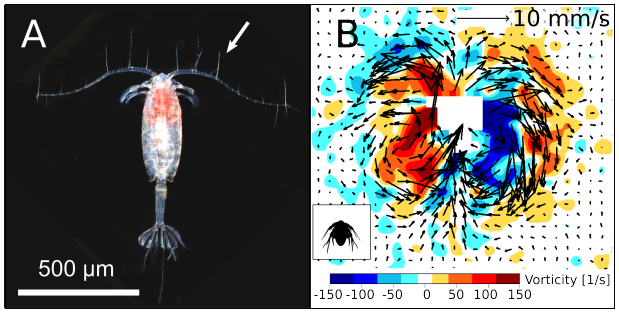


FIG. 2. **Mechanosensing. A:** Dorsal view of an adult *Acartia tonsa*, showing the antennules covered with mechanosensory setae, one of which is marked with an arrow (image courtesy of Erik Selander). **B:** Flow disturbance created by a swimming *Acartia tonsa* nauplius, visualized in the form of velocity vectors and vorticity contours.

## I. CHEMOSENSING

### A. A note on chemical contrast

An absolute upper limit on sensing range is dictated by the requirement of sufficient chemical contrast. Chemosensing requires spatial variations in signal strength that can be detected and gradients therein tracked. However, chemical gradients tend to become eroded with time to background level. The upper limit chemosensing range is not only related to the size and sensory ability of the organism, but also to the nature of the chemical substrate and its degradation in the environment due to microbial action or chemical reactions. Thus, while it is clear that an upper limit to chemosensing range exists, it is not possible to quantify it.

## II. VISION

### A. Size limit for compound eyes

The compound eye is hemi-spherical in shape and subdivided into light-detecting units called *ommatidia*. Ommatidia are conical in shape and cover the surface with an opening of width $\delta$. Given that the eye has a radius $r$, the visual acuity of an ommatidium is given by

$$\Delta\phi = \delta/r. \tag{1}$$

The number of ommatidia covering the hemispherical eye surface may be estimated as the ratio of the eye surface, around $2\pi r^2$, and the surface element covered by an ommatidium,

* erik.martens@sund.ku.dk
† nawa@fysik.dtu.dk

bioRxiv preprint doi: https://doi.org/10.1101/018937; this version posted September 15, 2015. The copyright holder for this preprint (which was not certified by peer review) is the author/funder. All rights reserved. No reuse allowed without permission.



around $r^2\Delta\phi^2$,

$$N = \frac{2\pi r}{\Delta\phi^2}. \tag{2}$$

Increasing the number of ommatidia, $N$, enlarges the image-resolution of the eye; however, as $\delta$ is decreases, diffraction effects becomes increasingly important. Thus, minimization of ommatidia in compound eyes is limited due to diffraction limits, see [1, 2]. Considering this trade-off, the optimal width of the ommatidia can be estimated [1], yielding

$$\delta = \sqrt{\lambda r}, \tag{3}$$

where $\lambda = 400$nm is the wave length of blue light.

Substituting Eqs. (1) and (3) into Eq. (2), we obtain the resolution of an eye with optimal ommatidia, we have

$$N = \frac{2\pi r}{\lambda}. \tag{4}$$

The size of an optimal compound eye is then

$$L_{\text{eye}} = 2r = \frac{\lambda N}{\pi}. \tag{5}$$

The size of the optimal compound eye with a reasonably useful resolution of $N = 100^2$ pixels should be $L_{\text{eye}} = 1.2$ mm, corresponding to roughly $L \sim 1$ to 3 cm (depending on the size ratio of eye to body). By comparison, some of the smallest organisms carrying compound eyes are *Daphnia*, with adults ranging from 1 to 5 mm [3]. Optimality of the eye, Eq. (5), then implies a resolution of $N \sim 10^2$ pixels – however, this is a resolution which barely produces a usable image.

### B. Sensing range

The sensing range condition in the main text is given by

$$C_0 e^{-\alpha R} \geq C_{\text{th,min}} + K R^2 L^{-4}. \tag{6}$$

Rescaling the sensing range, $\tilde{R} = \alpha R$ and the size, $\tilde{L} = (C_0\alpha^2/K)^{1/4}$ where $C := C_{\text{th,min}}/C_0$, this becomes

$$e^{-\tilde{R}} \geq C + \tilde{R}^2 \tilde{L}^{-4}. \tag{7}$$

The clear-water limit corresponds to small $\tilde{R} \ll 1$, yielding

$$\tilde{R} \sim \tilde{L}^2 (1 - C)^{1/2}, \tag{8}$$

and the turbid-water corresponds to large $\tilde{L}$, yielding

$$\tilde{R} \sim -\ln(C)/\alpha. \tag{9}$$

These expressions match the ones presented in the main text.

Letting the two expressions for the rescaled sensing ranges (8) and (9) be similar, we arrive at the condition for the crossover between the two regimes:

$$\tilde{L}_x^2 \sim -\ln(C)/(1 - C)^{1/2}, \tag{10}$$

which in the original unscaled variables becomes $L_{\text{x}}^2 \sim \alpha^{-1} K^{\frac{1}{2}} (C_0 - C_{\text{th,min}})^{-\frac{1}{2}} \ln(C_0/C_{\text{th,min}})$ or, to leading order,

$$L_{\text{x}}^2 \sim \alpha^{-1} K^{\frac{1}{2}} (C_0 - C_{\text{th,min}})^{-\frac{1}{2}}. \tag{11}$$

The clear-water limit occurs for $L \ll L_x$ and the turbid water limit for $L \gg L_x$. Thus, the turbid limit is reached in the limit of large $\alpha$, large $(C_0 - C_{\text{th,min}})$, or small sensitivity $K$, respectively.

Another (rough) estimate of the minimal body size, for which vision is still marginally meaningful, might be feasible from the condition that $L \sim R$ . This condition has at most two solutions, whereas the minimal solution is $L \approx [K/(C_0 - C_{\text{th,min}})]^{1/2}$. A precise determination of this estimate of the smallest animal carrying an eye is, however, difficult due to the unknown scaling coefficient in this estimate and uncertainties concerning parameter values.

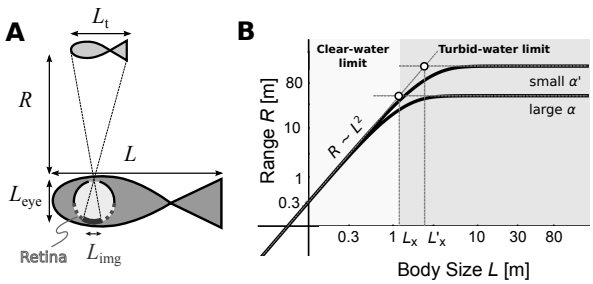


FIG. 3. **Vision. A**: An organism of body size $L$, with an eye of size $L_{\text{eye}}$, detects a target of size $L_t$ at a distance $R$ if the apparent contrast of the target is equal or larger than the threshold contrast of the organism's eye. **B**: Maximal visual sensing range scales with body size $L$: like $R \sim L^2$ in the clear-water limit ($L \ll L_x$) and like $R \sim$ constant in the turbid-water limit ($L \gg L_x$). Parameters are $C_0 = 0.3, C_{\text{th,min}} = 0.05$ (adopted from [4]), $K = 2.5 \times 10^{-4}$ m$^2$, $\alpha = 0.04$ m$^{-1}$ [5] (and $\alpha$' = 0.01 m$^{-1}$ for comparison).

## III. ECHOLOCATION

### A. Scaling argument for sensing range

We estimate how the range of echolocation scales with body size $L$ based on three assumptions: i) the threshold sensitivity of the ear $I_0$ is independent of organism size $L$ [6], ii) the emitted sound intensity $I_e$ scales with size: $I_e \propto L^{3\phi}$ where $3/4 < \phi < 1$, and iii) the carrier frequency of the signal depends on $L$ (see [7]).

The generated acoustic signal first travels through water, is then partially reflected by the target, and the remainder of the signal travels back to the organism. $I_e$, is thus reduced by two processes:

i) ***Reflection.*** The signal is reduced upon reflection from the target and the reflected intensity is proportional to the target area which scales as $L_{\text{t}}^2$.

ii) ***Attenuation.*** Sound intensity decreases with distance as $r^{-2}$ due to geometric divergence. It is further attenuated exponentially due to absorption in the seawater.

bioRxiv preprint doi: https://doi.org/10.1101/018937; this version posted September 15, 2015. The copyright holder for this preprint (which was not certified by peer review) is the author/funder. All rights reserved. No reuse allowed without permission.



Together, the signal intensity attenuates as $(2r)^{-2}e^{-2\mu r}$, where the factor 2 is due to the doubled travel distance. Geometric attenuation strongly dominates over the absorption processes, thus, $I_r \sim I_e L_t^2 r^{-2} \sim L^{3\phi} L_t^2 r^{-2}$. The strength of the returned signal must exceed the threshold intensity for detection in the ear, $I_r = I_0$, yielding a sensing range $R \sim I_0^{-1/2} L^{3\phi/2} L_\mathrm{t}$. Introducing the size ratio $p = L_\mathrm{t}/L$, we arrive at

$$R \sim p I_0^{-1/2} L^{\gamma}, \tag{12}$$

where the exponent $\gamma = 1 + 3\phi/2$ lies between 2.125 to 2.5. The scaling factor depends on unknown parameters, but can be estimated from data describing the echolocation range of small marine mammals. The resulting scaling coefficient (including $p/I_0$) is 6.47 $\mathrm{m}^{-1.5}$ for $\gamma = 2.5$, and 9.79 $\mathrm{m}^{-1.125}$ for $\gamma = 2.125$.

Figure 5 compares the scaling for Eq. 12 with data available for dolphins [8–12]. There is considerable scatter in the data, yet we recognize that the prediction compares with the data reasonably well.

### 1. *Signal attenuation*

We detail our estimates for the effects of attenuation due to geometric divergence and absorption processes in sea water. First, we discuss the effect of absorption processes on the transmission of pulses. To begin, we note that the absorption coefficient $\mu$ is frequency dependent. Each pulse is transmitted and characterized by its center (or carrier) frequency $f_c$, which is also the dominant frequency of the pulse spectrum. We may disregard all other frequencies and thus the dispersion of the transmitted pulse, leaving us with the task to find the absorption coefficient for $f_c$. The attenuation of sound in seawater is a complex molecular process which occurs both due to viscous absorption generated by particle motion, but also due to molecular relaxation processes by Boric acid and Magnesium sulphate. A formula for the frequency dependent absorption has been devised [13]. However, this relation is too complicated for our purposes as we desire to establish a simple asymptotic scaling relation between $f_c$ and $\mu$; indeed, the data is well *parameterized* by $\mu \sim f_c^{4/3}$ (see Section 3 below and Figure 5). Further, it is known that $f_c$ depends on body size; experimental data [7] for dolphins (excluding river dolphins), allows us to heuristically deduce a scaling dependence for the absorption, $f_c \approx 370\ \mathrm{m}^{3/4}\ \mathrm{s}^{-1} \times L^{-3/4}$ (see Section 2 below). Combining these two scalings, we obtain for the absorption coefficient (decibel / meter) $\mu \approx 10^{-2} L^{-1}$. Finally, since the fitted data is measured in the logarithmic decibel scale, the attenuation factor due to absorption converts to $10^{-0.1\mu(L)\times 2R}$. Summed up, the intensity is reduced by a factor $I_r/I_e \sim R^{-2} 10^{-0.001\times 2R/L}$. However, further analysis shows that the effect of damping is negligible when compared to the geometric divergence. Thus, the reflected sound intensity simplifies to $I_r \sim L^{3\phi} L_o^2 R^{-2}$.

### 2. *Center frequency*

Center frequencies of echolocation signals have been measured for dolphins [7], shown in Figure 4A. The two river dolphins discussed in [7] are excluded from our analysis, since dolphins in such environments operate at different frequencies to adapt for sound transmission in non-free environments. We fitted the relation between the body mass $w$ and the center frequency by $f_c \approx (368.7\ \mathrm{m}^{0.26}\ \mathrm{s}^{-1}) \times m^{-0.26}$. Since the mass scales as $w \sim L^3$, we obtain $f_c \sim L^{-3/4}$.

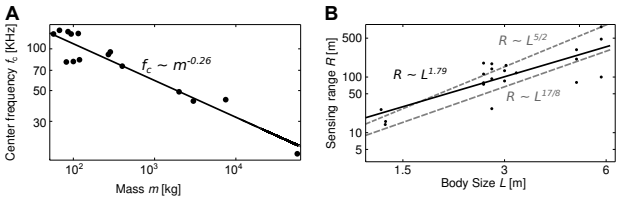


FIG. 4. **Echolocation.** **A:** Power law fit for echolocation center frequencies of dolphins. Data from [7]: $f_c$ = (17.5, 42, 43, 75, 49, 95, 83.4, 80.4, 91, 81, 128, 136, 129, 133, 128) kHz; $m$ = (57000, 3000, 7500, 400, 2000, 285, 119, 82, 270, 100, 94, 67.5, 115, 86, 57) kg. **B:** Comparison of the predicted echolocation sensing range (dashed grey) with data (black dots), which scales like $R \approx 14.2\ \mathrm{m}^{-0.79} \cdot L^{1.79}$ (black line, least squares fit).

For comparison, note that the frequency with maximal intensity produced in the nasal sac is approximated by the Helmholtz frequency [14]:

$$f_p = \frac{c}{2\pi}\left(\frac{A}{V\ L_\mathrm{t}}\right)^{1/2} \propto L^{-1}. \tag{13}$$

where $A$, $V$, $L_\mathrm{t}$ are the area, volume and length of the nasal sac. Given that $m$ is proportional to $L^3$, the scaling observed in Fig. 4 appears to deviate somewhat from this theoretical estimate. The deviation may be explained by shortcomings of the simple Helmholtz oscillator model.

### 3. *Sound absorption in marine environments*

The authors in [13] derive a simplified equation of the form

$$\mu = A_1 P_1 f_1 f_c^2/(f_1^2 + f_c^2) + A_2 P_2 f_2 f_c^2/(f_2^2 + f_c^2) + A_3 P_3 f_c^2 \tag{14}$$

where the center frequency $f_c$ is measured in Hz at the depth $z$ in km. Further, they determine the following coefficients characteristic to the properties of seawater for boron and for magnesium,

$$\begin{aligned} f_1 &= 0.78 * (S/35)^{1/2} e^{T/26} \\ f_2 &= 42 e^{T/17} \\ A_1 &= 0.106 \\ A_2 &= 0.52 * (1 + T/43)(S/35) \\ A_3 &= 0.00049 \\ P_1 &= e^{(pH-8)/0.56} \end{aligned}$$

bioRxiv preprint doi: https://doi.org/10.1101/018937; this version posted September 15, 2015. The copyright holder for this preprint (which was not certified by peer review) is the author/funder. All rights reserved. No reuse allowed without permission.



$$P_2 = e^{-z/6}$$
$$P_3 = e^{-(T/27+z/17)}.$$

| Location | pH | S [ppt] | T [C] | z [km] |
|---|---|---|---|---|
| Pacific | 7.7 | 34 | 4 | 1 |
| Red Sea | 8.2 | 40 | 22 | 0.2 |
| Arctic Ocean | 8.2 | 30 | -1.5 | 0 |
| Baltic Sea | 7.9 | 8 | 4 | 0 |

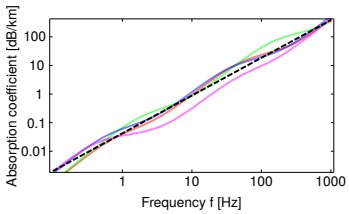


FIG. 5. Power law fit for relation between frequency and sound absorption coefficient in the ocean. **Top:** Parameter values for $pH, S, T, z$ for Eq. 14 valid for different ocean regions. **Bottom:** Absorption rates resulting from parameters for the various regions listed in the top table. Fitting the logarithmic data linearly (dashed line) over the frequency range of interest results in the asymptotic scaling relation $\mu$ [db/km] $\approx 0.0434\ \mathrm{s}^{-4/3}\mathrm{km}^{-1} \times f^{4/3}[\mathrm{s}^{-1}]$.

The scaling for the absorption coefficient $\mu$ is thus (decibel per meter)

$$\mu \approx 4.2 \times 10^{-5}\mathrm{s}^{4/3}\mathrm{m}^{-1} \times f_c^{4/3}. \tag{15}$$

where the center frequency ($\mathrm{s}^{-1}$) is

$$f_c \approx 65.8\,\mathrm{s}^{-1}\mathrm{m}^{3/4} \times L^{-3/4} \tag{16}$$

where we have used the relation mass w = $\rho L^3$ with $\rho = 10^3$ kg m$^{-3}$. Thus, we obtain (decibel per meter)

$$\mu \approx 10^{-2} \times L^{-1}. \tag{17}$$

### B. Assumptions underlying the scaling argument

The scaling argument for the range rests on assumptions supported by data only in part, which we review here for clarity:

(A1) the threshold sensitivity of the ear $I_0$ is independent of target size $L$. This approximation is supported by audiograms (behavioral and auditory brain stem responses) of odontocetes [12, 15–18],

(A2) the emitted sound intensity that an animal produces scales with size: $I_e \propto L^{3\phi}$ where $3/4 < \phi < 1$,

(A3) the carrier frequency of the sonar signal depends on size $L$.

Assumption (A3) seems fairly well corroborated, as already discussed in section A and B. Assumption (A2) states that the scaling exponent $\phi$ is allowed to vary in a small range corresponding to a sublinear volume dependence of the generating organ size which is a fairly reasonable assumption. Taking into account the considerable scatter of the data, we recognize that the prediction compares with the data reasonably well, as is evidenced in Figure 7 in the main text. However, better data is required to further underpin assumption (A1). Indeed, within the group of whales and dolphins we find no clear *size*-dependence for the sensitivity threshold $I_0$ [18]; but it would be desirable to obtain more data to solidify this assumption, as well as to identify a satisfactory physical or biological explanation for why the sensitivity is independent of body size, in contrast to other mammal groups [15–19].


[1] R. P. Feynman. Color vision. In Michael A. (Caltech) Gottlieb and Rudolf (Caltech) Pfeiffer, editors, *The Feynman Lectures on Physics*, chapter 36.4. California Institute of Technology, 2013.

[2] MF Land. Visual acuity in insects. *Annual Review of Entomology*, 42(46):147–177, 1997.

[3] Dieter Ebert. *Ecology, Epidemiology, and Evolution of Parasitism in Daphnia*. Bethesda (MD): National Center for Biotechnology Information (US), 2005.

[4] RL Dunbrack and DM Ware. Energy constraints and reproductive trade-offs determining body size in fishes. In P. Calow, editor, *Evolutionary Physiological Ecology*, pages 191–218. Cambridge University Press, 1987.

[5] Aike Beckmann and Inga Hense. Beneath the surface: Characteristics of oceanic ecosystems under weak mixing conditions – a theoretical investigation. *Progress in Oceanography*, 75(4):771–796, December 2007.

[6] D. R. Ketten. Marine mammal auditory systems: A summary of audiometric and anatomical data and implications for underwater acoustic impacts. *Polarforschung*, 72(2/3):79–92, 2004.

[7] Frants H Jensen, Alice Rocco, Rubaiyat M Mansur, Brian D Smith, Vincent M Janik, and Peter T Madsen. Clicking in shallow rivers: Short-range echolocation of irrawaddy and ganges river dolphins in a shallow, acoustically complex habitat. *PloS one*, 8(4):e59284, January 2013.

[8] WWL Au and KJ Snyder. Long-range target detection in open waters by an echolocating atlantic bottlenose dolphin (tursiopstruncatus). *The Journal of the Acoustical Society of* . . . , pages 1077–1084, 1980.

[9] Lance G Barrett-Lennard, John K Ford, and Kathy A Heise. The mixed blessing of echolocation: Differences in sonar use by fish-eating and mammal-eating killer whales. *Animal Behaviour*, 51:553–565, 1996.

[10] R A Kastelein, W W Au, H T Rippe, and N M Schooneman. Target detection by an echolocating harbor porpoise (phocoena phocoena). *The Journal of the Acoustical Society of America*, 105:2493–2498, 1999.

[11] A. Earl Murchison. *Animal Sonar Systems*. Springer US, Boston, MA, January 1980.

[12] J. Teilmann, L. A. Miller, T. Kirketerp, R. A. Kastelein, P. T. Madsen, B. K. Nielsen, and W. L. Au. Characteristics of echolocation signals used by a harbour porpoise (*Phocoena phocoena*) in a target detection experiment. *Aquatic Mammals*,

bioRxiv preprint doi: https://doi.org/10.1101/018937; this version posted September 15, 2015. The copyright holder for this preprint (which was not certified by peer review) is the author/funder. All rights reserved. No reuse allowed without permission.



28:275–284, 2002.

[13] MA Ainslie and JG McColm. A simplified formula for viscous and chemical absorption in sea water. *The Journal of the Acoustical Society of America*, 103(June 1997):1997–1998, 1998.

[14] JL Aroyan, MA McDonald, SC Webb, JA Hildebrand, D Clark, JT Laitman, and JS Reidenberg. Acoustic models of sound production and propagation. In *Hearing by Whales and Dolphins*, number 2000. 2000.

[15] Paul E. Nachtigall, T. Aran Mooney, Kristen a. Taylor, and Michelle M. L. Yuen. Hearing and auditory evoked potential methods applied to odontocete cetaceans. *Aquatic Mammals*, 33(1):6–13, January 2007.

[16] A F Pacini, P E Nachtigall, L N Kloepper, M Linnenschmidt, A Sogorb, and S Matias. Audiogram of a formerly stranded long-finned pilot whale (globicephala melas) measured using auditory evoked potentials. *The Journal of Experimental Biology*, 213:3138–3143, 2010.

[17] Aude F Pacini, Paul E Nachtigall, Christopher T Quintos, T David Schofield, Dera a Look, Gregg a Levine, and Jason P Turner. Audiogram of a stranded blainville's beaked whale (mesoplodon densirostris) measured using auditory evoked potentials. *The Journal of Experimental Biology*, 214(Pt 14):2409–15, July 2011.

[18] DOSITS.org. What sounds can animals hear? *Discovery of Sound in the Sea (dosits.org)*, 2014.

[19] R. A. Kastelein, P. Bunskoek, M. Hagedoorn, W. L. Au, and D. de Haan. Audiogram of a harbor porpoise (phocoena phocoena) measured with narrow-band frequency-modulated signals. *The Journal of the Acoustical Society of America*, 112(1):334, 2002.